

FRACTURE BEHAVIOUR OF Fe₃Al ALLOY WITH ADDITIONS OF Zr AND C AT DIFFERENT TEMPERATURES

JAKUB PRAHL¹, PETR HAUŠILD¹, MIROSLAV KARLÍK^{1*},
JEAN-FRANÇOIS CRENN^{1,2}

¹*Czech Technical University in Prague, Faculty of Nuclear Sciences and Physical Engineering, Department of Materials, Trojanova 13, 120 00 Praha 2, Czech Republic*

²*Université de Bretagne-Sud, Laboratoire de Génie Mécanique et Matériaux, Rue de Saint-Maudé, BP92116, 56321 Lorient, France*

Received 12 October 2004, accepted 7 January 2005

The static and fatigue behaviour of hot rolled Fe-31.5Al-3.5Cr [at.%] with addition of zirconium and carbon was studied at different temperatures. The tensile deformation tests were carried out at temperatures ranging from 20 to 600 °C. The fatigue crack growth rate ($v\text{-}\Delta K$) curves were measured at 20, 300 and 500 °C. The best fatigue crack growth resistance was reached at 300 °C, while at 500 °C the crack growth rate was the highest and the fatigue life the shortest. The predominant fatigue fracture mechanism is transgranular cleavage. However, a number of other micromorphologic features corresponding to various fracture mechanisms were observed: transgranular quasi-cleavage facets, ductile fatigue striations and brittle striations.

When tested at high temperatures, the fracture surface in the zone of static rupture contained signs of plastic deformation, whose amount increased with increasing temperature.

Key words: iron aluminides, fracture micromechanisms, fractography, fatigue crack growth

1. Introduction

Alloys based on Fe-Al (iron aluminides) rank to the most studied intermetallics particularly because of their low price, low density, good wear resistance, relatively easy fabrication and high corrosion resistance in oxidizing and sulfidizing environments. For these advantages the iron aluminides were supposed to replace steels and other alloys in specific applications such as heating elements, furnace fixtures,

*corresponding author, e-mail: karlik@kmat.fjfi.cvut.cz

heat exchangers and many others. However, there have been also two main disadvantages limiting their use – low ductility at ambient temperature and low strength at elevated temperatures [1–3]. Mechanical properties, especially yield strength, are influenced by the change of order ($D0_3 \leftrightarrow B2$ order-order transition) at temperature of about 540 °C [4]. Low ductility was characterized as an extrinsic effect caused by water vapour from surrounding atmosphere (hydrogen embrittlement) [5, 6]. However, it has been shown, that a sufficient room temperature (RT) tensile elongation (10 to 20 %) and tensile yield strength as high as 500 MPa at 600 °C can be reached through a control of composition and microstructure [2]. Many alloying elements were used to improve the properties of Fe₃Al alloys (Cr, Si, Ce, B, Zr, Y, Nb, W, etc.). Increasing of tensile strength was noted for additions of Mo, Nb, Ti, Si or Zr. Molybdenum and niobium decrease the RT ductility [7, 8], however chromium increases the RT ductility with almost no effect on the strength and fatigue properties [9, 10], zirconium and carbon show a beneficial effect on the crack growth resistance [11, 12].

The purpose of this paper is to investigate the effect of Zr and C addition on tensile and fatigue properties of Fe-31.5Al-3.5Cr [at.%) alloy at room and elevated temperatures.

2. Experimental

An alloy with nominal composition of Fe-31.5Al-3.5Cr-0.25Zr-0.2C [at.%) was prepared by vacuum induction melting and casting. The ingot was hot rolled at 1100 °C to a plate 7 mm thick (reduction in thickness 75 %) and subsequently quenched into mineral oil. Results of the chemical analysis of the alloy are in Table 1. After machining by milling, all the test specimens were annealed in air at 700 °C for 2 hours to relieve internal stresses and then quenched into mineral oil. The microstructure of the material was recovered, with elongated grains having up to 1 mm in the direction of rolling and up to 300 μm in the transverse direction (Fig. 1).

Static tensile tests were carried out at temperatures 20 (RT), 200, 300, 400, 500, and 600 °C respectively on INSTRON 1195 testing machine equipped with a resistance-heated furnace. At each temperature, two cylindrical specimens having 3 mm in diameter and 22 mm gauge length were tested at the constant crosshead speed of 2 mm/min (initial strain rate $1.6 \times 10^{-3} \text{ s}^{-1}$).

Table 1. Chemical composition of the alloy

	Al	Cr	Zr	C	Fe
[at.%)	31.46	3.5	0.25	0.19	Balance
[wt.%)	18.2	3.9	0.49	0.05	Balance

Fatigue crack growth experiments were performed on compact tension (CT) specimens of thickness $B = 5$ mm and width $W = 40$ mm. The notch was prepared by electro-discharge cutting using a wire 0.2 mm in diameter. The initial crack length a_0 was 6.5 mm. The fatigue crack propagated perpendicularly to the rolling direction. The specimens were loaded in tension at 20, 300 and

500 °C on a computer-controlled servohydraulic loading machine INOVA ZUZ 50 equipped with a resistance-heated furnace. The frequency of loading was 10 Hz, the stress ratio R was 0.042 and the maximum load was 4.8 kN. The crack length during fatigue test was measured by (temperature independent) potential method at alternative current with the frequency of 4 Hz, using TECHLAB SRT-2K device, controlled by Fatigue Crack Growth Monitor software.

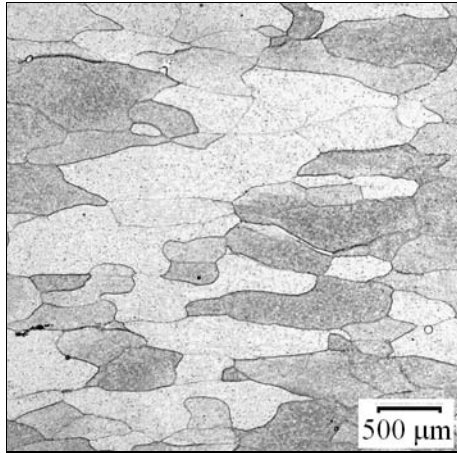


Fig. 1. Microstructure of Fe-28Al-3.5Cr-0.25Zr-0.2C [at.%] alloy showing elongated grains in the rolling direction.

Scanning electron microscope JEOL JSM 840A was used for the fractographic analysis. Micrographs were taken in the magnification range 10–20,000 \times .

3. Results and discussion

3.1 Tensile tests

The basic mechanical characteristics, 0.2% proof stress ($R_{p0.2}$), ultimate tensile strength (R_m) and tensile elongation (A), were measured at six different temperatures. Average values are listed in Table 2 and plotted in Fig. 2.

Temperature dependence of $R_{p0.2}$ and R_m in Fig. 2 shows some local extremes. Considering the range from 20 °C to 540 °C (D0₃ region), both characteristics have their minimum at 200 °C, while the maximum values are reached at 300 °C (R_m) and 500 °C ($R_{p0.2}$), respectively. In both cases, measured values at 20 °C and 500 °C

Table 2. Tensile mechanical properties of studied material

	20 °C	200 °C	300 °C	400 °C	500 °C	600 °C
$R_{p0.2}$ [MPa]	503	413	691	621	551	362
R_m [MPa]	350	184	280	261	362	330
A [%]	3.6	11.5	13.6	10.3	17.2	35.0

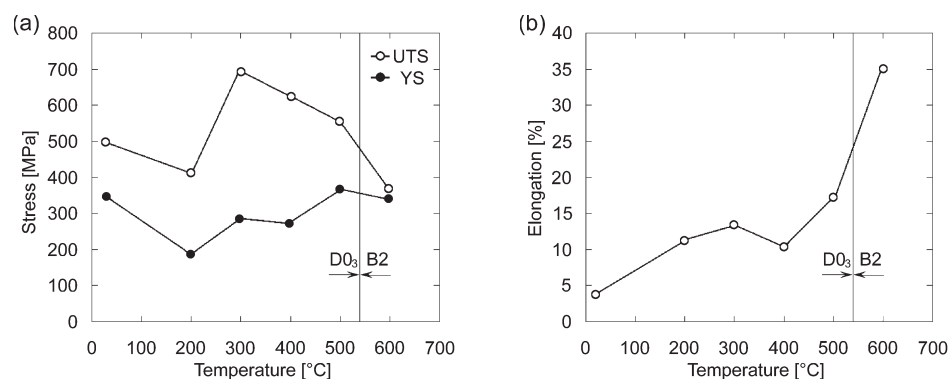


Fig. 2. Temperature dependence of the 0.2% proof stress, ultimate strength (a) and elongation (b).

are comparable and the values of $R_{p0.2}$ and R_m at 600°C (B2 region) are practically identical. Tensile elongation at elevated temperatures is 3 to 4 times higher than tensile elongation at room temperature. In D0₃ region the elongation slightly increased with temperature, except for 400°C, where the value dropped down to 10%. At 600°C, in B2 region, the elongation was substantially higher than at 500°C (D0₃ region) (Fig. 2b).

These data can be compared with recent results measured on similar materials – Fe-28Al-3.6Cr-0.1Ce-0.16C [at.%] alloy in the form of an extruded tube [4] and Fe-28Al-3.2Cr-0.01Ce-0.16C [at.%] hot rolled plate [13].

Temperature dependences in Fig. 2 are very similar to these from [4]. Mechanical behaviour of the material from extruded tube differs only a little at RT, where it exhibits an elongation of 6.5% and 8.5% for strain rates $\sim 10^{-4} \text{ s}^{-1}$ and $\sim 10^{-2} \text{ s}^{-1}$, respectively. Our material, tested at strain rate $\sim 10^{-3} \text{ s}^{-1}$, shows elongation only 3.6%. This difference could be caused by much higher grain size ($\sim 1 \text{ mm}$ – Fig. 1) in comparison to [4] ($\sim 100 \text{ }\mu\text{m}$). If we compare present results with those from [13], the temperature dependences of $R_{p0.2}$ and R_m as well as the separate values are in a good agreement. The only difference consists in evolution of elongation with temperature. While in [13] the elongation after reaching its maximum value at 300°C (11.5%) drops at 500°C approximately to the same value as at RT ($\sim 2.5\%$), in the present study the elongation is higher (17.2%) at 500°C than the RT and 300°C values.

Fracture surfaces of tensile specimens broken at different temperatures are shown in Fig. 3. With increasing temperature, there is an apparent increase of plastic deformation preceding the fracture (see reduction in fracture area in Fig. 3).

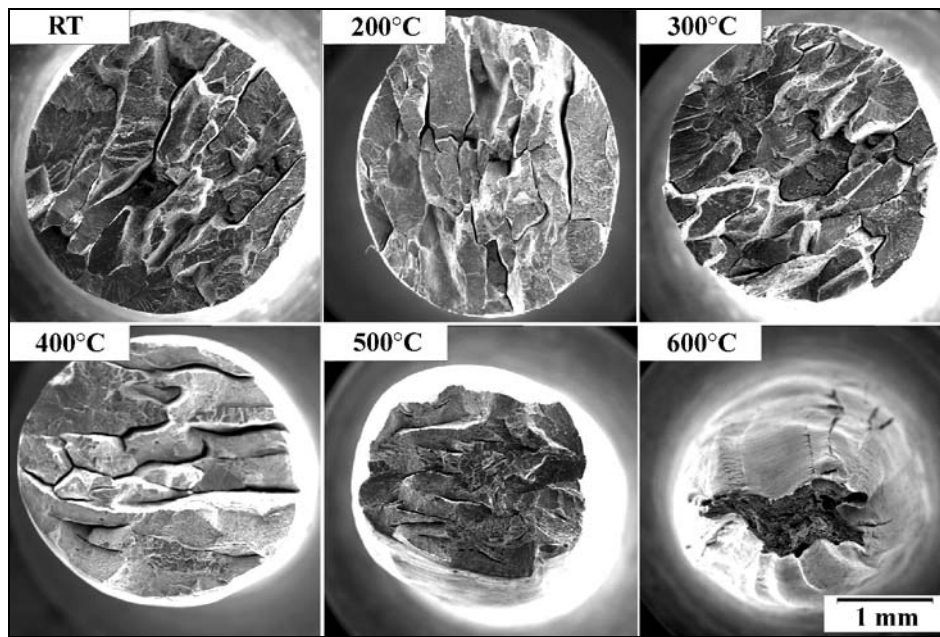


Fig. 3. Fracture surfaces of tensile specimens broken at different temperatures.

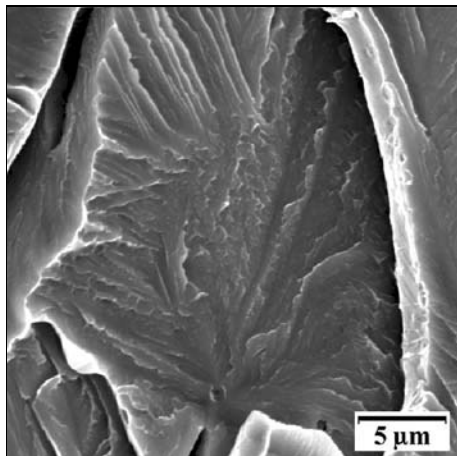


Fig. 4. Cleavage facets on the fracture surface (static rupture at 200°C).

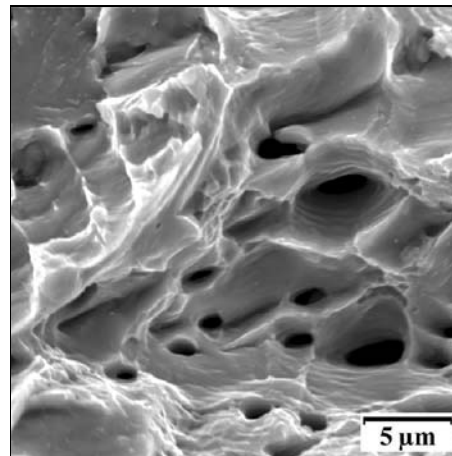


Fig. 5. Ductile dimples on the fracture surface (static rupture at 600°C).

Another characteristic feature is the presence of large intergranular cracks following the rolling direction and oriented perpendicularly to the fracture surface (Fig. 3). The opening of these intergranular cracks seems to grow with increasing temperature up to 400°C. Fracture mechanism changed from transgranular cleavage (Fig. 4) at RT to entirely ductile dimpled fracture (Fig. 5) at 600°C.

3.2 Fatigue tests

The crack length a was measured during the fatigue tests as a function of elapsed number of loading cycles N . The fatigue crack growth rate $v = da/dN$, determined by the secant method, is plotted in Fig. 6 as a function of the stress intensity factor range ΔK (calculated for the corresponding crack length a).

Firstly, it is possible to see significant difference of slopes in v - ΔK plot (exponent n in Paris equation) between the curves corresponding to 20°C and that

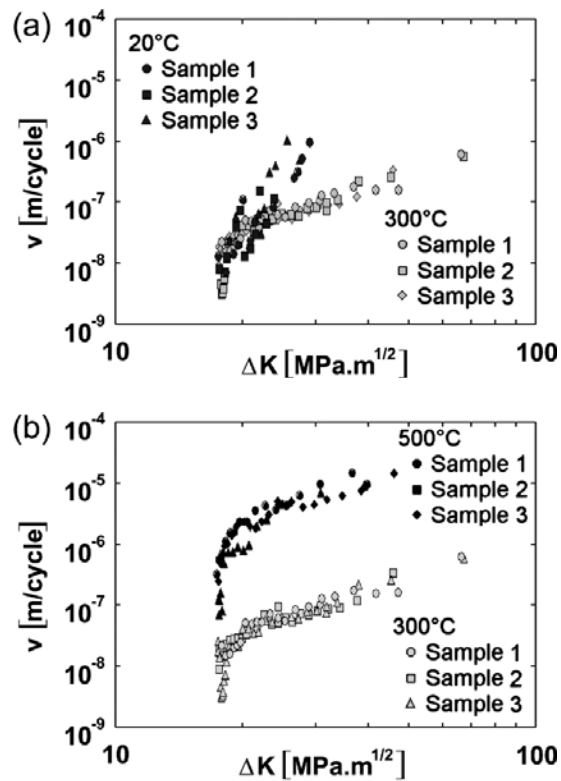


Fig. 6. Fatigue crack growth (v - ΔK) plots for specimens tested (a) at 20°C and 300°C, (b) at 300°C and 500°C.

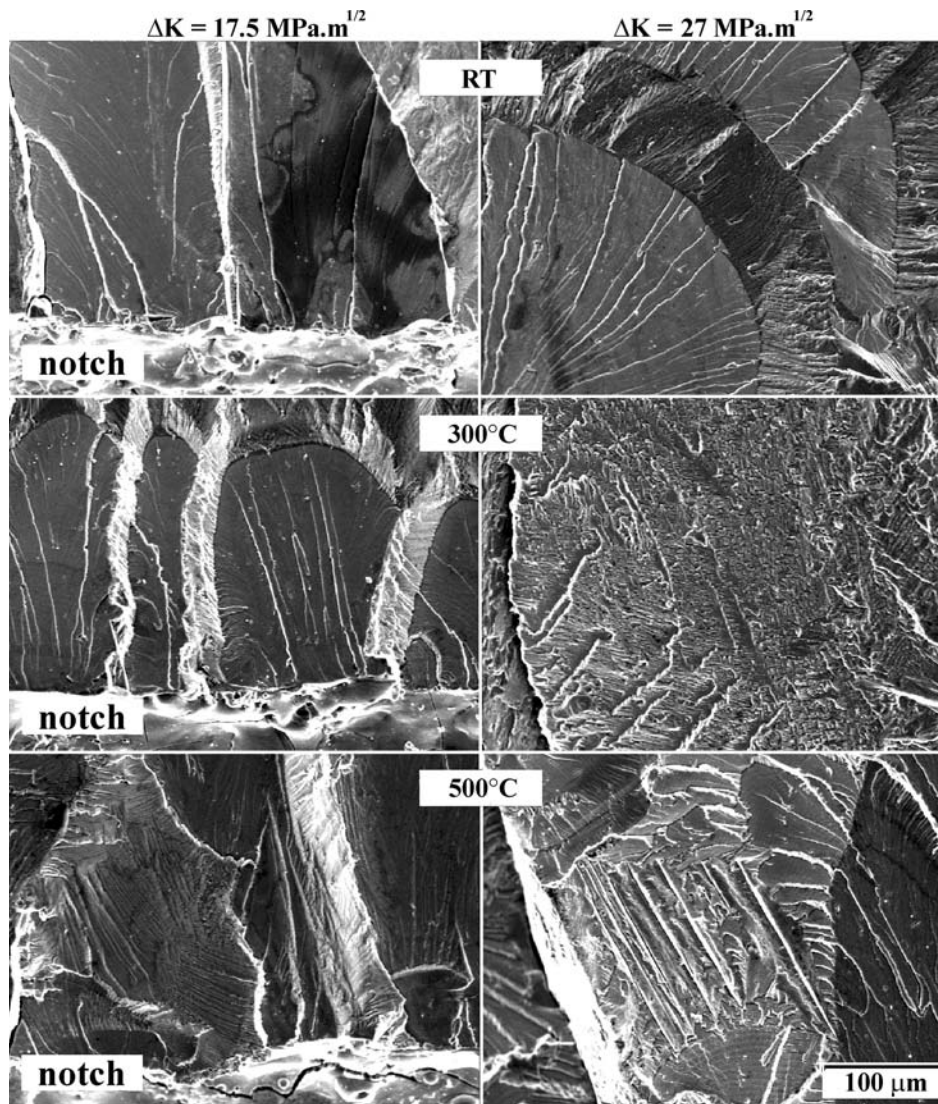


Fig. 7. Fatigue fracture surfaces at different temperatures and ΔK . Left column – $\Delta K = 17.5 \text{ MPa} \cdot \text{m}^{1/2}$ close to the notch, right column – $\Delta K = 27 \text{ MPa} \cdot \text{m}^{1/2}$.

of 300°C. The similar change of n (about four times higher at RT than at 300°C) was observed as well in [13] but there was a point of intersection of the two curves (for ΔK of about $24 \text{ MPa} \cdot \text{m}^{1/2}$), while in the graph presented in Fig. 3a, it seems that both curves start at the same threshold value of ΔK (about $17 \text{ MPa} \cdot \text{m}^{1/2}$).

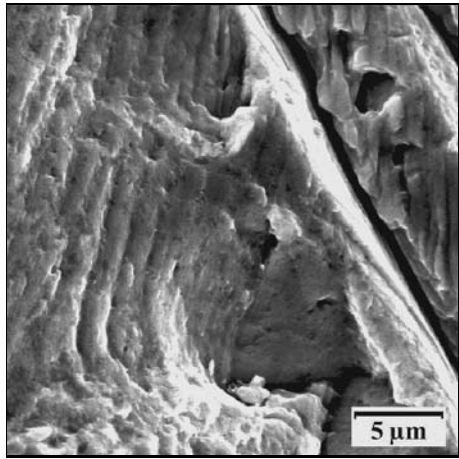


Fig. 8. Ductile striations formed on the fatigue fracture surface (500°C).

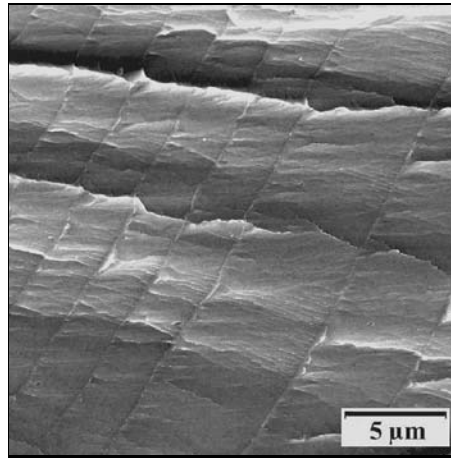


Fig. 9. Brittle striations found on a cleavage facet (RT).

When tested at 500°C, the crack growth rate values were almost 100 times higher (for the same values of ΔK) than at 300°C, while the slopes in v - ΔK plot were practically the same. The results are in a good agreement in comparison to the results presented in [13]. The only difference is that the curves in graphs presented here are slightly shifted to the right (higher values of ΔK – the upper estimate of threshold value of ΔK is $17 \text{ MPa}\cdot\text{m}^{1/2}$ while it was $15.6 \text{ MPa}\cdot\text{m}^{1/2}$ in [13]). This is probably a consequence of alloying by zirconium [10, 11]. The fatigue behaviour at elevated temperature is in accordance with literature [14].

Number of cycles to failure was measured for each fatigue test at each applied temperature. Although the longest fatigue lives were reached by the specimens tested at room temperature (approx. 245,000 cycles), specimens tested at 300°C ruptured in average after 228,000 cycles (except one whose fatigue life was more than 300,000 cycles). When tested at 500°C, the fatigue life rapidly decreased to approx. 6,000 cycles. The drop of number of cycles to failure when changing the test temperature from 300 to 500°C is in agreement with results presented in [13].

The character of the fatigue fracture surfaces of specimens tested at different temperatures is presented in Fig. 7. The main fracture micromechanism is transgranular cleavage. There were no important changes in character of morphology of fatigue fracture surface with increasing the test temperature or with increasing the stress intensity factor (compare the left and right column in Fig. 7).

Although the fracture surface consisted particularly of irregular cleavage facets, other morphologic features corresponding to different fracture mechanisms were

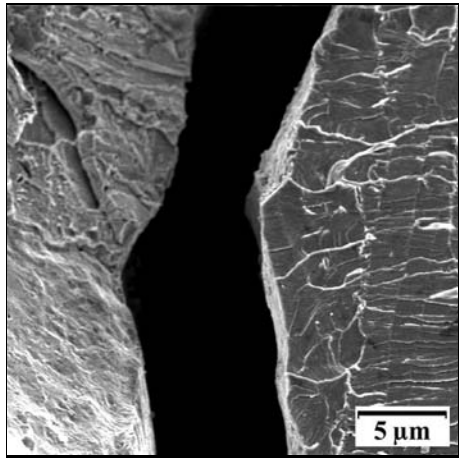


Fig. 10. Intergranular crack found in the zone of the final rupture (500°C).

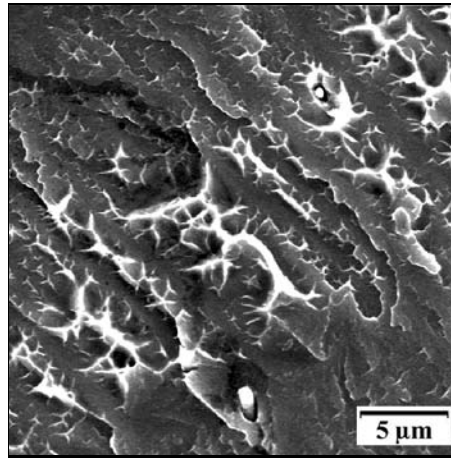


Fig. 11. Signs of plastic deformation during the final fracture (300°C).

found: transgranular quasi-cleavage facets, ductile dimpled rupture, intergranular decohesion, ductile fatigue striations formed by Laird's mechanism [15] (Fig. 8) and brittle striations resulting from cyclic cleavage (Fig. 9). The brittle striations formed striation fields frequently orientated perpendicularly to the main crack growth direction. The spacing between striations did not correspond to expected global crack growth rate in observed area.

In the regions of final (static) rupture, large intergranular cracks (Fig. 10) orientated perpendicularly to the fracture surface were found, similarly as in the case of tensile tests. The character of fracture surface changed with temperature from transgranular cleavage (at RT) to ductile dimpled fracture (at 500°C). An increasing amount of plastic deformation in the zone of static rupture is shown in Fig. 11. The observed micromorphological features as well as fracture mechanisms were similar to those reported in [13].

4. Conclusions

The static and fatigue behaviour of hot rolled Fe-31.5Al-3.5Cr [at.%] with additions of zirconium and carbon was characterized at room and elevated temperatures.

The maximum value of 0.2% proof stress was reached at 500°C, the maximum value of tensile strength at 300°C. The elongation increased with temperature, except for 400°C, when its value dropped down to 10%. At 600°C (in B2 region), the elongation was substantially higher (35%) than the highest value in D0₃ region

(17 % measured at 500 °C). Fracture surfaces of broken tensile specimens changed from transgranular cleavage facets at RT to entirely ductile dimpled fracture at 600 °C.

The fatigue crack growth rate ($v\text{-}\Delta K$) curves were measured at RT, 300 °C and 500 °C. The highest fatigue crack growth resistance was found at 300 °C. At 500 °C, the crack growth rate was substantially higher and there was a rapid decrease of fatigue life. In comparison to the recent experiments [13], the alloying by zirconium is beneficial for fatigue life by increasing the threshold value of stress intensity factor.

In the region of fatigue fracture, the main micromechanism is transgranular cleavage at all studied temperatures. Besides the transgranular cleavage, transgranular quasi-cleavage facets, ductile fatigue striations and brittle striations were also found on fatigue fracture surfaces.

In the region of final fracture, there is a significant increase of signs of plastic deformation with increasing temperature. Similarly as on static fracture surfaces of broken tensile specimens it is possible to see a continuous change of fracture mechanisms from transgranular cleavage at 20 °C to ductile dimpled fracture at 500 °C.

Acknowledgements

Financial support from the Czech Science Foundation (Project ‘Improvement of properties of Fe₃Al based intermetallics by thermomechanical treatment and by modified compositions’ – GA CR 106/02/0687) is gratefully acknowledged.

REFERENCES

- [1] McKAMEY, C. G.—DEVAN, J. H.—TORTORELLI, P. F.—SIKKA, V. K.: *J. Mater. Res.*, 6, 1991, p. 1779.
- [2] DEEVI, S. C.—SIKKA, V. K.: *Intermetallics*, 4, 1996, p. 357.
- [3] SAUTHOFF, G.: *Intermetallics*. Weinheim, Verlag Chemie 1995.
- [4] KARLÍK, M.—KRATOCHVÍL, P.—JANEČEK, M.—SIEGL, J.—VODIČKOVÁ, V.: *Mater. Sci. Eng.*, A289, 2000, p. 182.
- [5] ALVEN, D. A.—STOLOFF, N. S.: *Scripta Mater.*, 34, 1996, p. 1937.
- [6] CASTAGNA, A.—STOLOFF, N. S.: *Mater. Sci. Eng.*, A192/193, 1995, p. 399.
- [7] LIU, C. T.—McKAMEY, C. G.—LEE, E. H.: *Scripta Metall. Mater.*, 24, 1989, p. 385.
- [8] LYNCH, R. L.—HELDT, L. A.—MILLIGAN, W. W.: *Scripta Metall. Mater.*, 25, 1991, p. 2147.
- [9] LYNCH, R. L.—GEE, K. A.—HELDT, L. A.: *Scripta Metall. Mater.*, 30, 1994, p. 945.
- [10] STOLOFF, N. S.: In: *Physical Metallurgy and Processing of Intermetallic Compounds*. Eds.: Stoloff, N. S., Sikka, V. K. New York, Chapman & Hall 1996, p. 489.
- [11] STOLOFF, N. S.—ALVEN, D. A.—McKAMEY, C. G.: In: *International Symposium on Nickel and Iron Aluminides*. Eds.: Deevi, S. C. et al. Warrendale, ASM International 1997, p. 65.

- [12] ALVEN, D. A.—STOLOFF, N. S.: *Mater. Sci. Eng.*, A239–240, 1997, p. 362.
- [13] HAUŠILD, P.—KARLÍK, M.—NEDBAL, I.—PRAHL, J.: *Kovove Mater.*, 42, 2004, p. 156.
- [14] STOLOFF, N. S.—CASTAGNA, A.—SCOTT, J.—DUQUETTE, D. J.: In: *Processing, Properties and Application of Iron Aluminides*. Eds.: Schneibel, J. H., Crimp, M. A. Warrendale, The Minerals, Metals & Materials Society 1994, p. 271.
- [15] LAIRD, C.: In: *Fatigue Crack Propagation*. Am. Soc. Test. Mater., Spec. Tech. Publ., 415, 1967, p. 131.